Strange and charm contributions to nucleon charges and moments[*]

Rui Zhang,[a,b,*] **Tanmoy Bhattacharya,**[c] **Rajan Gupta,**[c] **Huey-Wen Lin,**[a,b] **Santanu Mondal,**[c] **Sungwoo Park**[c] **and Boram Yoon**[c]

[a]*Department of Physics and Astronomy, Michigan State University, East Lansing, MI 48824*

[b]*Department of Computational Mathematics, Science and Engineering, Michigan State University, East Lansing, MI 48824*

[c]*Computer, Computational, and Statistical Sciences CCS-7, Los Alamos National Laboratory, Los Alamos, NM 87545, USA*

E-mail: zhangr60@msu.edu

We present preliminary results for strange and charm contributions to nucleon charges and moments. The scalar, axial and tensor charges, and unpolarized first moments are calculated using clover-on-HISQ formulation and cover four lattice spacings, $a = \{0.06, 0.09, 0.12, 0.15\}$ fm, and three pion masses, $M_\pi = \{310, 220, 130\}$ MeV. The renormalization factors are calculated non-perturbatively using the RI-sMOM scheme. We carry out a chiral and continuum extrapolation to obtain physical results.

The 38th International Symposium on Lattice Field Theory, LATTICE2021 26th-30th July, 2021
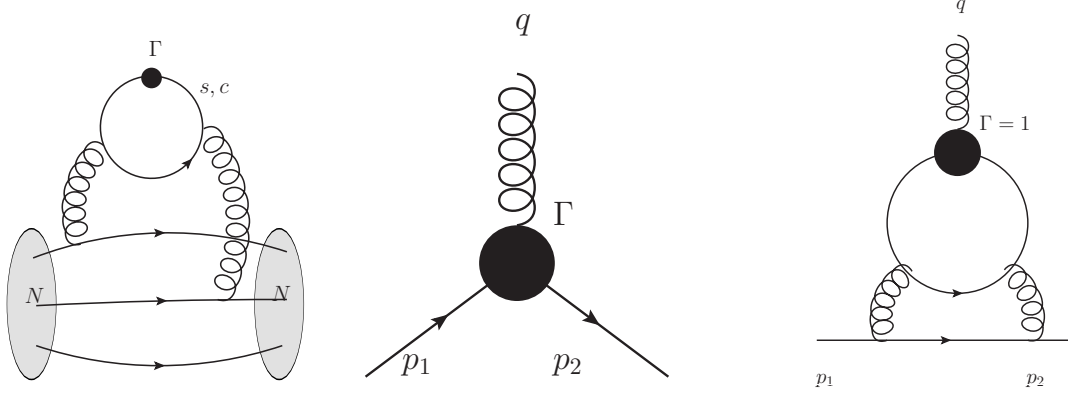*Zoom/Gather@Massachusetts Institute of Technology*

Figure 1: Left: Disconnected diagram on lattice. Connected NPR diagrams (Middle) for all operators and mixing diagrams (right) for the scalar charge.

1. Introduction

Nucleon charges and moments are important quantities to study for the elucidation of the nucleon structure. The scalar charge plays an important role in dark matter search, and gives the pion-nucleon sigma term. The axial charge is the contribution of quark spins to the proton spin, and enters in the spin-dependent dark matter cross-section. The tensor charge gives the contribution of the quark Electric Dipole Moment (EDM) to the neutron EDM. The first unpolarized moment gives the momentum fraction of the quark, an important quantity to describe the quark PDF especially for sea quarks. These quantities for the isovector $(u - d)$ case have been calculated with high precision using lattice QCD. As the precision of light quark calculation improves, the contributions from heavier quark flavors, strange and charm, also need to be precisely determined.

All operators for charge and moment calculations are quark bilinears, $O = \bar{q}\Gamma q$. Specifically, for the charge operators, $\Gamma = \mathbf{1}$ for the scalar charge, $\Gamma = \gamma_i \gamma_5$ for the axial charge, $\Gamma = \sigma_{ij}$ for the tensor charge, are local operators. On the other hand, $\Gamma = D_4 \gamma_4 - \frac{1}{3} \sum_i D_i \gamma_i$ is a non-local operator for the first unpolarized moment, which gives the momentum fraction carried by the quark.

For strange and charm quarks, the contribution only comes from disconnected diagrams, ie, the correlation of the self contraction of the quark bilinear operator $\bar{q}\Gamma q$ (forming a quark loop) with the nucleon, as shown in Fig. 1. The details of disconnected calculations can be found in Ref. [4].

2. Lattice Setup, Matrix Elements and Renormalization

We calculated 2- and 3-point functions on six ensembles generated with 2+1+1 flavors of highly improved staggered quarks (HISQ) [5] by the MILC collaboration [6]. They cover four lattice spacings, $a \approx \{0.06, 0.09, 0.12, 0.15\}$ fm, and 3 pion masses of $M_\pi \approx \{130, 220, 310\}$ MeV. To reduce statistical noise, the lattices are hypercubic (HYP) smeared [7] before the calculation of the quark propagators. The details of the ensembles are summarized in Table 1. We computed the nucleon two point correlators of the nucleon interpolating operator χ with different projections $\mathcal{P}$:

$$C_{2pt}^{\mathcal{P}}(\tau) = \langle 0|\mathcal{P}\chi(\tau)\bar{\chi}(0)|0\rangle, \tag{1}$$

a (fm)	M_π (MeV)	$L^3 \times T$	N_{conf}^c	N_{conf}^s	N_{src}^c	N_{src}^s	$\frac{N_{\text{src}}^{2pt}}{\text{cfg}}$
0.06	320(2)	$48^3 \times 144$	469	87	4000	4000	32
0.09	313(3)	$32^3 \times 96$	633	889	6000	6000	32
0.09	138(1)	$64^3 \times 96$	721	310	4000	4000	32
0.12	310(3)	$24^3 \times 64$	983	897	4000	8000	32
0.12	228(2)	$32^3 \times 64$	902	869	5000	5000	32
0.15	321(4)	$16^3 \times 48$	n/a	1795	n/a	2000	32

Table 1: Parameters of the 2+1+1-flavor HISQ ensembles used for the strange and charm contributions to the nucleon charges and moments. N_{conf} gives the number of gauge configurations, N_{src} is the number of the noise source measurements to approximate the disconnected loop propagators, and $\frac{N_{\text{src}}^{2pt}}{cfg}$ is the number of the two-point sources on each configuration.

where $\mathcal{P}^{\text{unp}} = (1 + \gamma_4)/2$ for unpolarized projection, and $\mathcal{P}^{\text{pol}} = (1 + \gamma_4)(1 + i\gamma_5\gamma_i)/2$ for polarized projection. Then we compute the disconnected loops:

$$C_{\text{loop}}^O = \sum_n \text{Tr}\left[\hat{O}S(n)\right] \tag{2}$$

These two are combined together to obtain the disconnected contribution.

$$C_{3\text{pt}}^O(t,\tau) = \left\langle \left(C_{2\text{pt}}^{\mathcal{P}}(\tau) - \langle C_{2\text{pt}}^{\mathcal{P}}(\tau)\rangle\right)\left(C_{\text{loop}}^O(t) - \langle C_{\text{loop}}^O(t)\rangle\right)\right\rangle$$

We make 2-state fits to the correlators using their spectral decomposition:

$$C_{2\text{pt}}^{\mathcal{P}^{unp}}(\tau) = |A_0|^2 e^{-E_0\tau} + |A_1|^2 e^{-E_1\tau} \tag{3}$$

$$C_{3\text{pt}}^O(t,\tau) = \Big(|A_0|^2\langle 0|O|0\rangle e^{-E_0 t}e^{-E_0(\tau-t)} + A_0 A_1\langle 1|O|0\rangle e^{-E_0 t}e^{-E_1(\tau-t)} +$$
$$A_1 A_0\langle 0|O|1\rangle e^{-E_1 t}e^{-E_0(\tau-t)} + |A_1|^2\langle 1|O|1\rangle e^{-E_1 t}e^{-E_1(\tau-t)}\Big) \tag{4}$$

to extract the ground state matrix elements $\langle 0|O|0\rangle$. The fit results are displayed in Fig. 2 along with the data for the ratio of 3-point to 2-point functions, $R(t,\tau) = C_{3\text{pt}}^O(t,\tau)/C_{2\text{pt}}^{\mathcal{P}^{unp}}(\tau)$. The fit results are consistent with the data points.

To renormalize the matrix elements, we used the regularization-independent symmetric momentum subtraction (RI-sMOM) scheme. In this scheme, we choose symmetric momentum configurations for the external quark state and the momentum transfer $p_1^2 = p_2^2 = (p_2 - p_1)^2 = \mu_R^2$, as shown in the middle panel of Fig. 1. They are then matched to $\overline{MS}$ scheme using 2-loop perturbation theory, and run to $\mu = 2$ GeV. The μ_R-dependence is then removed by fitting the Z-factors to $Z_\Gamma(\mu) = Z_\Gamma + c_1\mu_R^2 + c_2\mu_R^4$. The renormalization for the scalar charge and the momentum fraction is more complicated. The momentum fraction for quarks mixes with other flavors as well as gluons, which is not included in our work so far. The scalar charge also mixes with other flavors, as shown in the right of Fig. 1, and we have included the mixing between strange quark and light iso-scalar combination, but not for the charm quark so far. The two diagrams for calculating Z_S are done for
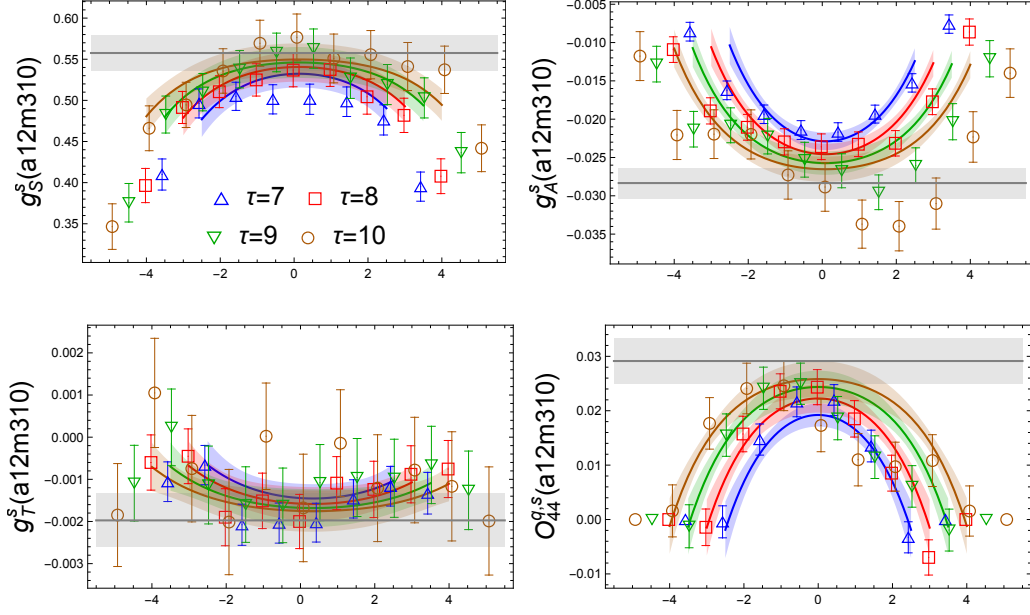
Figure 2: Ratio plots from lattice data (colored markers) and the reconstructed ratio from 2-state fit results (colored bands) on the a12m310 ensemble. The gray bands label the ground state matrix elements.

all the flavor combinations as the connected ($c_{ff'}$) and disconnected ($d_{ff'}$) parts:

$$c_{ff'} \equiv \frac{\delta_{ff'}}{12 Z_\psi^f} \operatorname{Tr}\left[\langle f | O^{f'} | f \rangle_{\text{conn}}\right], \quad d_{ff'} \equiv \frac{-1}{12 Z_\psi^f} \operatorname{Tr}\left[\langle f | O^{f'} | f \rangle_{\text{disc}}\right]. \tag{5}$$

Using these, we renormalize the bare charges in the following way:

$$\begin{pmatrix} g_S^{R,u+d} \\ g_S^{R,s} \\ g_S^{R,c} \end{pmatrix} = \begin{pmatrix} c_l - 2d_{ll} & -2d_{sl} & -2d_{cl} \\ -d_{ls} & c_s - d_{ss} & -d_{cs} \\ -d_{lc} & -d_{sc} & c_c - d_{cc} \end{pmatrix}^{-1} \cdot \begin{pmatrix} g_S^{\text{bare},u+d} \\ g_S^{\text{bare},s} \\ g_S^{\text{bare},c} \end{pmatrix} \tag{6}$$

Note that $d_{ff'}$ is sensitive to the flavor in the quark loop, f', but insensitive to the external quark f.

3. Chiral and Continuum Extrapolation

After renormalization, we obtain the charges and momentum fraction on different ensembles. The results for strange quark are shown in Fig. 3, and those for charm quark are shown in Fig. 4. We extrapolate these quantities to the physical point by fitting to the ansatz:

$$g(M_\pi, a) = g^{\text{phy}}(1 + c_i a^i + d_2(M_\pi^2 - (M_\pi^{\text{phy}})^2)), \qquad i = 1, 2, \tag{7}$$

for linear ($i = 1$) or quadratic ($i = 2$) dependence on the lattice spacing.

The extrapolations linear (quadratic) in lattice spacing are shown as magenta (purple) bands in Fig. 5 and Fig. 6 for strange quark results. We notice that the M_π dependence is non-negligible while the a dependence in g_A, g_T, O_{44}^S is not clear. The a dependence is large in g_S. The linear
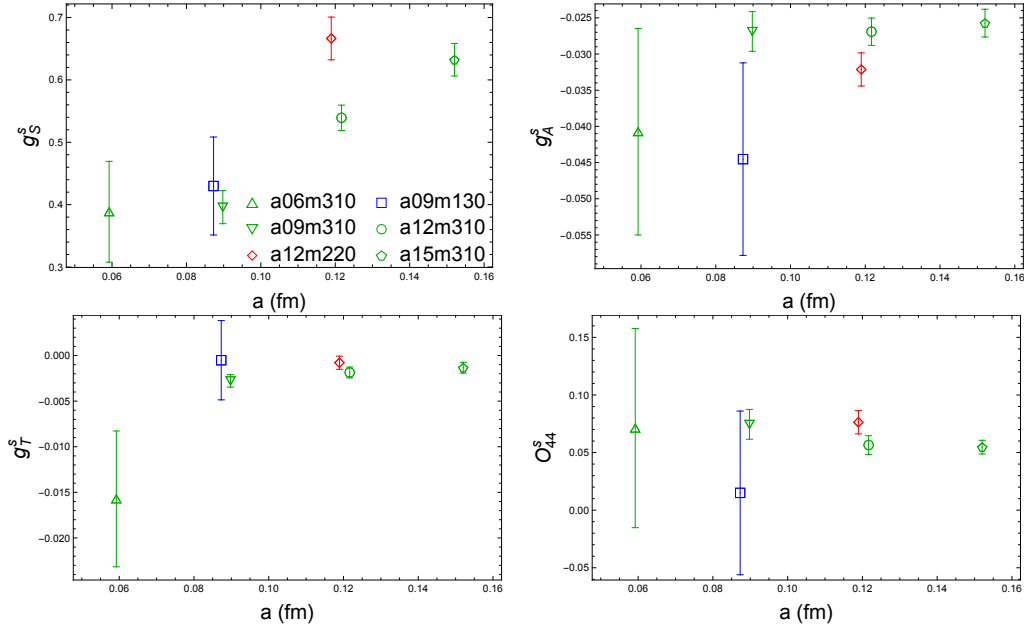
Figure 3: Renormalized charges and momentum fraction for the strange quark.
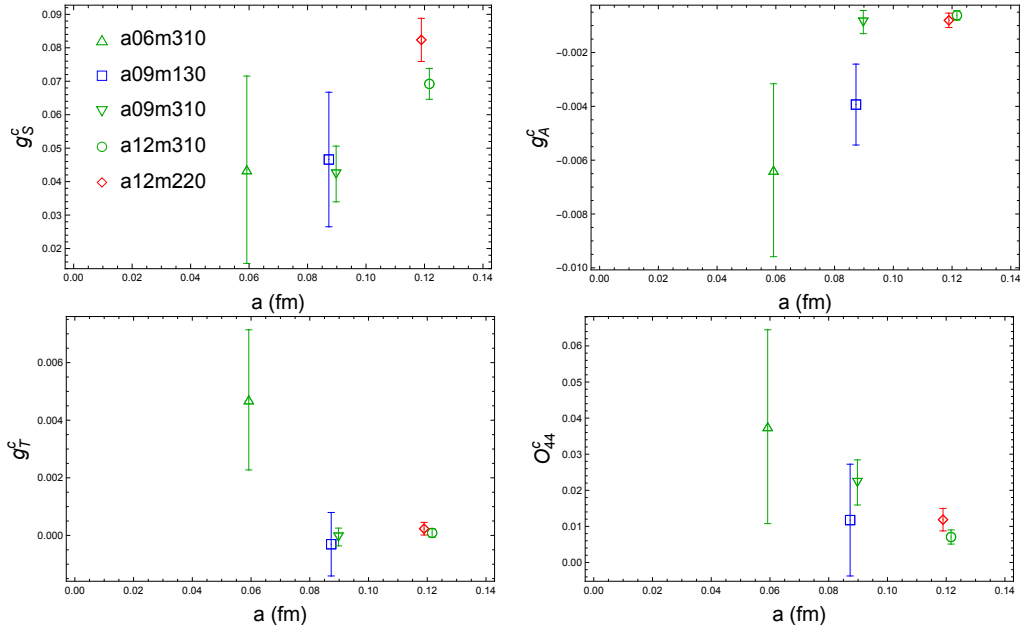

Figure 4: Renormalized charges and momentum fraction for the charm quark.
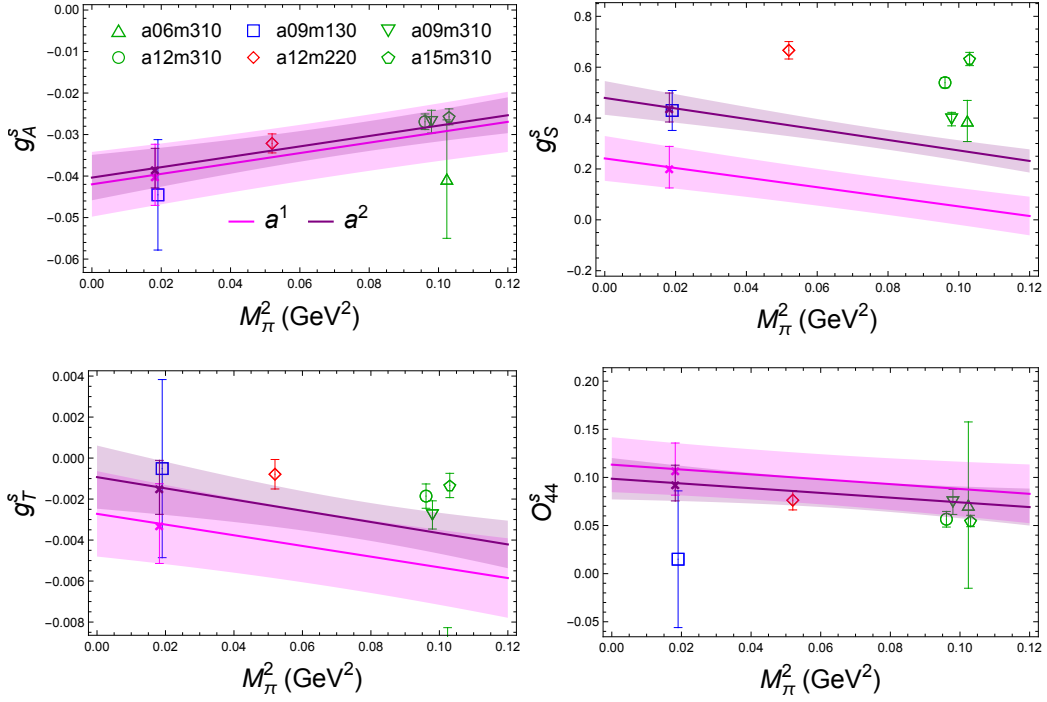
Figure 5: Chiral and continuum extrapolation of strange contribution to charges and momentum fraction using Eq. (7), and shown as a function of M_π^2 with $a = 0$.
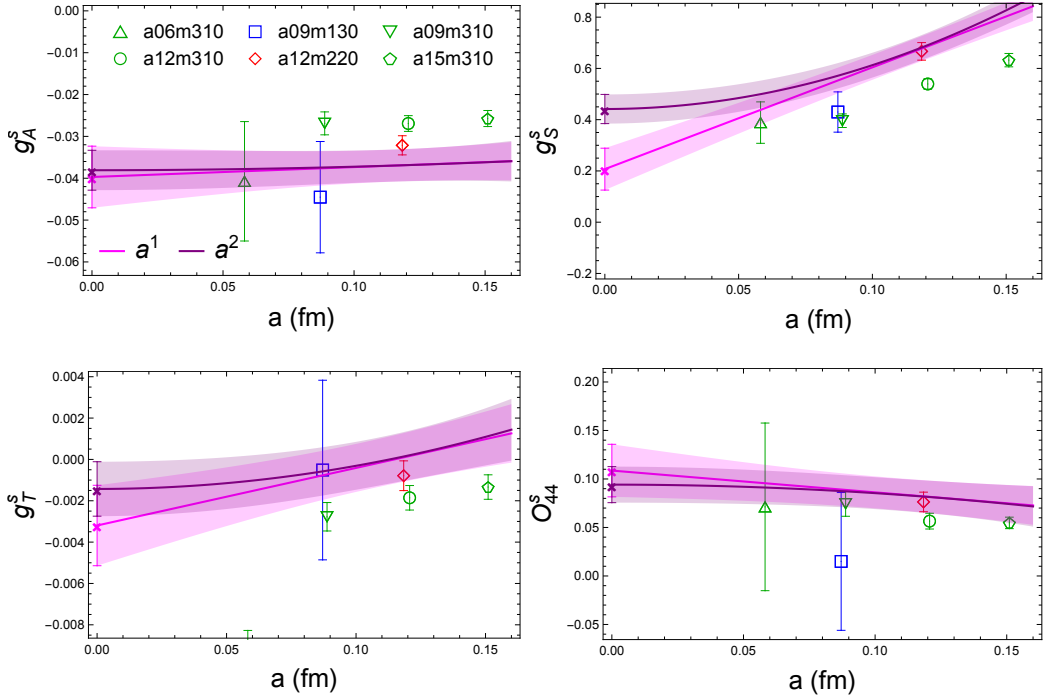

Figure 6: Chiral and continuum extrapolation of strange contribution to charges and momentum fraction using Eq. (7), and shown as a function of lattice spacing with M_π set to 135 MeV.
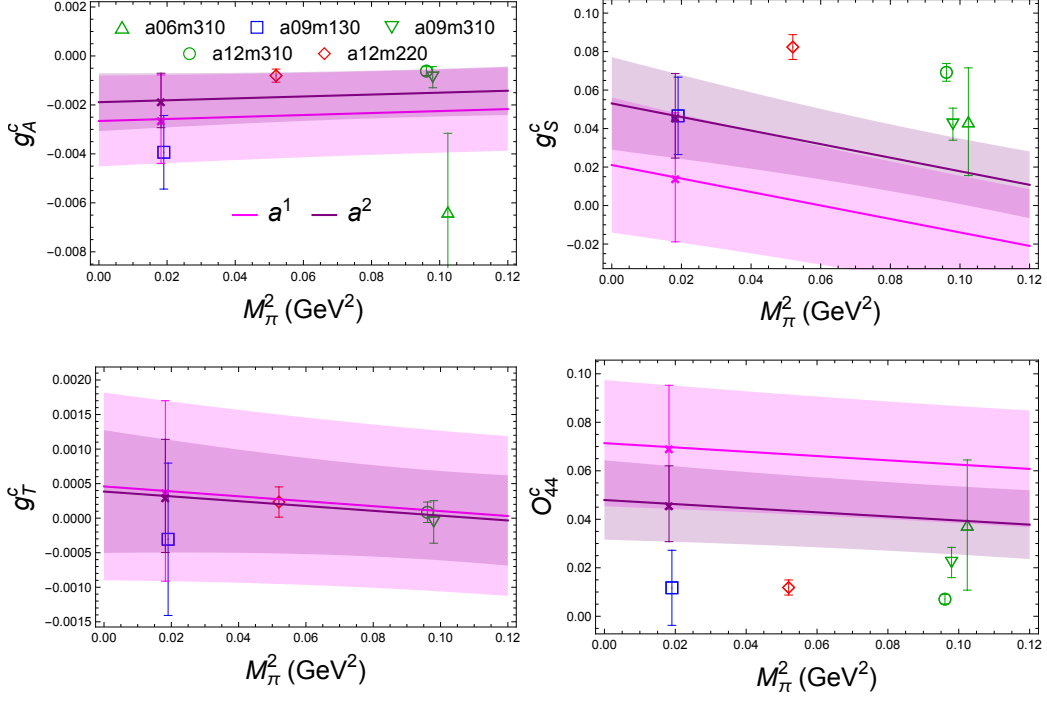
Figure 7: Chiral and continuum extrapolation of charm contribution to charges and momentum fraction using Eq. (7), and shown as a function of M_π^2 with $a = 0$.

and quadratic fits have similar χ^2 and the two results are consistent within 1σ except for g_S. We are working on improving the statistics on finer lattices to better constrain the extrapolation.

The extrapolations linear (quadratic) in lattice spacing are shown as magenta (purple) bands in Fig. 7 and Fig. 8 for charm quark results. Unlike the strange results, the M_π dependence is not significant for charm. The a and a^2 extrapolations are consistent within 1σ. We also note that the scalar charge reduces under continuum extrapolation, while the momentum fraction becomes larger under continuum extrapolation.

Comparison is made with previous results in Tab. 2 for the strange quark and in Tab. 3 for the charm quark. We find that the axial and tensor charges are consistent with previous results. Our scalar charge has large uncertainty because of the smaller statistics on finer lattices. The momentum fraction (without including mixing correction) is much larger.

4. Conclusion

In this work, we present the calculation of strange and charm contribution to nucleon charges and momentum fraction. We computed the disconnected diagrams on 6 lattice ensembles covering 4 lattice spacings and 3 pion masses that allow us to extrapolate to the physical point. The renormalization constants are calculated in the RI-sMOM scheme and then matched to $\overline{MS}$ scheme and evolved to $\mu = 2$ GeV. We take into account the mixing for scalar charge between strange and iso-scalar, but have not included the mixing for momentum fractions. Our results on axial charge and tensor charge are consistent with previous lattice results. The scalar charge calculation needs increased statistics on finer lattices. The calculation of momentum fraction also needs more data and the evaluation of mixing with gluon operator and other flavors.
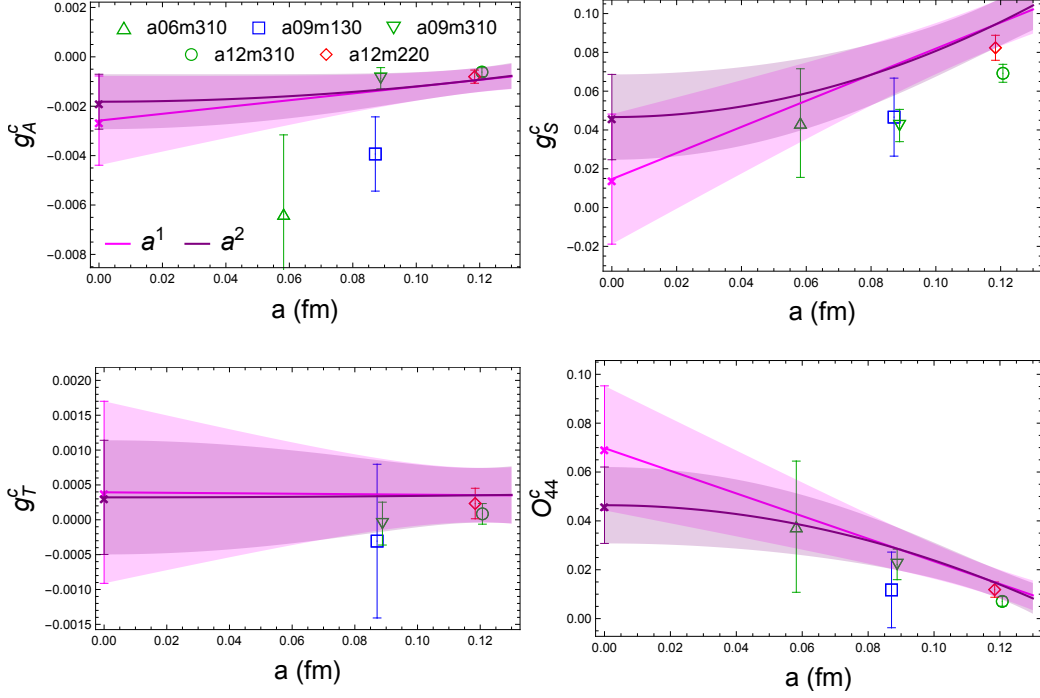
Figure 8: Chiral and continuum extrapolation of charm contribution to charges and momentum fraction using Eq. (7), and shown as a function of lattice spacing, with M_π set to 135 MeV.

strange	$g_S^{s,R}$	$g_A^{s,R}$	$g_T^{s,R}$	$\langle x \rangle_s$
This work (preliminary)	$0.13 \sim 0.50$	$-0.0397(73)$	$-0.0032(19)$	$0.109(27)$
PNDME'18 [8, 9]	n/a	$-0.053(8)$	$-0.0027(16)$	n/a
★ETMC'19 [10, 11] Nf=4	$0.454(16)$	$-0.0458(73)$	$-0.00268(58)$	$0.052(12)$
★ETMC'19 [10] Nf=2	$0.371(38)$	$-0.061(17)$	$-0.0041(12)$	n/a
χQCD'18 [12, 13]	n/a	$-0.035(9)$	n/a	$0.051(26)$
★JLQCD'18 [14]	$0.15(16)$	$-0.046(28)$	$-0.012(18)$	n/a

Table 2: Comparison of our strange quark results with previous calculations of the same quantities. Results labeled with ★ are from single lattice spacing.

charm	$g_S^{c,R}$	$g_A^{c,R}$	$g_T^{c,R}$	$\langle x \rangle_c$
This work (preliminary)	$0.015(34)$	$-0.0026(18)$	$0.0004(13)$	$0.070(25)$
★ETMC'19 Nf=4	$0.075(17)$	$-0.0098(34)$	$-0.00024(16)$	$0.019(9)$
★ETMC'19 Nf=2	$0.059(18)$	$-0.0065(51)$	$-0.0060(37)$	n/a

Table 3: Comparison of our charm quark results with previous calculations of the same quantities. Results labeled with ★ are from single lattice spacing.

References

[1] **SciDAC, LHPC, UKQCD** Collaboration, R. G. Edwards and B. Joo, *The Chroma software system for lattice QCD*, *Nucl. Phys. Proc. Suppl.* **140** (2005) 832, [hep-lat/0409003]. [,832(2004)].

[2] R. Babich, J. Brannick, R. Brower, M. Clark, T. Manteuffel, S. McCormick, J. Osborn, and C. Rebbi, *Adaptive multigrid algorithm for the lattice Wilson-Dirac operator*, *Phys. Rev. Lett.* **105** (2010) 201602, [arXiv:1005.3043].

[3] J. Osborn, R. Babich, J. Brannick, R. Brower, M. Clark, S. Cohen, and C. Rebbi, *Multigrid solver for clover fermions*, *PoS* **LATTICE2010** (2010) 037, [arXiv:1011.2775].

[4] **PNDME** Collaboration, T. Bhattacharya, V. Cirigliano, S. Cohen, R. Gupta, A. Joseph, H.-W. Lin, and B. Yoon, *Iso-vector and Iso-scalar Tensor Charges of the Nucleon from Lattice QCD*, *Phys. Rev. D* **92** (2015), no. 9 094511, [arXiv:1506.06411].

[5] **HPQCD, UKQCD** Collaboration, E. Follana, Q. Mason, C. Davies, K. Hornbostel, G. P. Lepage, J. Shigemitsu, H. Trottier, and K. Wong, *Highly improved staggered quarks on the lattice, with applications to charm physics*, *Phys. Rev. D* **75** (2007) 054502, [hep-lat/0610092].

[6] **MILC** Collaboration, A. Bazavov et al., *Lattice QCD Ensembles with Four Flavors of Highly Improved Staggered Quarks*, *Phys. Rev. D* **87** (2013), no. 5 054505, [arXiv:1212.4768].

[7] A. Hasenfratz and F. Knechtli, *Flavor symmetry and the static potential with hypercubic blocking*, *Phys. Rev. D* **64** (2001) 034504, [hep-lat/0103029].

[8] R. Gupta, B. Yoon, T. Bhattacharya, V. Cirigliano, Y.-C. Jang, and H.-W. Lin, *Flavor diagonal tensor charges of the nucleon from (2+1+1)-flavor lattice QCD*, *Phys. Rev. D* **98** (2018), no. 9 091501, [arXiv:1808.07597].

[9] H.-W. Lin, R. Gupta, B. Yoon, Y.-C. Jang, and T. Bhattacharya, *Quark contribution to the proton spin from 2+1+1-flavor lattice QCD*, *Phys. Rev. D* **98** (2018), no. 9 094512, [arXiv:1806.10604].

[10] C. Alexandrou, S. Bacchio, M. Constantinou, J. Finkenrath, K. Hadjiyiannakou, K. Jansen, G. Koutsou, and A. Vaquero Aviles-Casco, *Nucleon axial, tensor, and scalar charges and σ-terms in lattice QCD*, *Phys. Rev. D* **102** (2020), no. 5 054517, [arXiv:1909.00485].

[11] C. Alexandrou, S. Bacchio, M. Constantinou, J. Finkenrath, K. Hadjiyiannakou, K. Jansen, G. Koutsou, H. Panagopoulos, and G. Spanoudes, *Complete flavor decomposition of the spin and momentum fraction of the proton using lattice QCD simulations at physical pion mass*, *Phys. Rev. D* **101** (2020), no. 9 094513, [arXiv:2003.08486].

[12] Y.-B. Yang, J. Liang, Y.-J. Bi, Y. Chen, T. Draper, K.-F. Liu, and Z. Liu, *Proton Mass Decomposition from the QCD Energy Momentum Tensor*, *Phys. Rev. Lett.* **121** (2018), no. 21 212001, [arXiv:1808.08677].

[13] J. Liang, Y.-B. Yang, T. Draper, M. Gong, and K.-F. Liu, *Quark spins and Anomalous Ward Identity*, *Phys. Rev. D* **98** (2018), no. 7 074505, [arXiv:1806.08366].

[14] **JLQCD** Collaboration, N. Yamanaka, S. Hashimoto, T. Kaneko, and H. Ohki, *Nucleon charges with dynamical overlap fermions*, *Phys. Rev. D* **98** (2018), no. 5 054516, [arXiv:1805.10507].